Electronic Supplementary Material (ESI) for RSC Advances.

Supporting information for

Discovery of Novel 1,2,4-Triazole Tethered β-Hydroxy Sulfides as Bacterial Tyrosinase Inhibitors: Synthesis and Biophysical Evaluation through In vitro and In silico Approaches

Table of Contents

1- ^{1}H and ^{13}C NMR spectra of compounds **11a-h**

2- Bacterial tyrosinase Inhibition

1- ^{1}H and ^{13}C NMR spectra of compounds **11a-h**

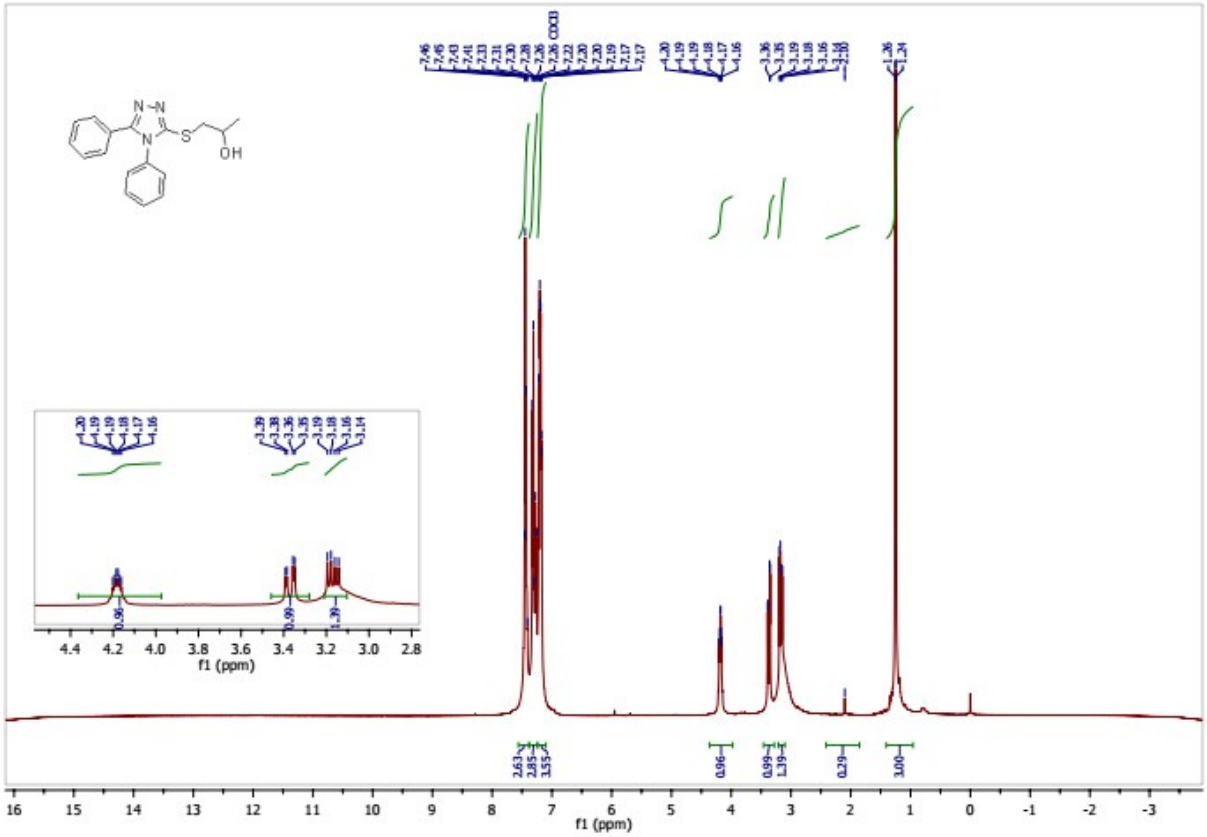

Figure S1: ^{1}H NMR spectrum of 1-((4,5-diphenyl-4*H*-1,2,4-triazol-3-yl)thio)propan-2-ol (**11a**).

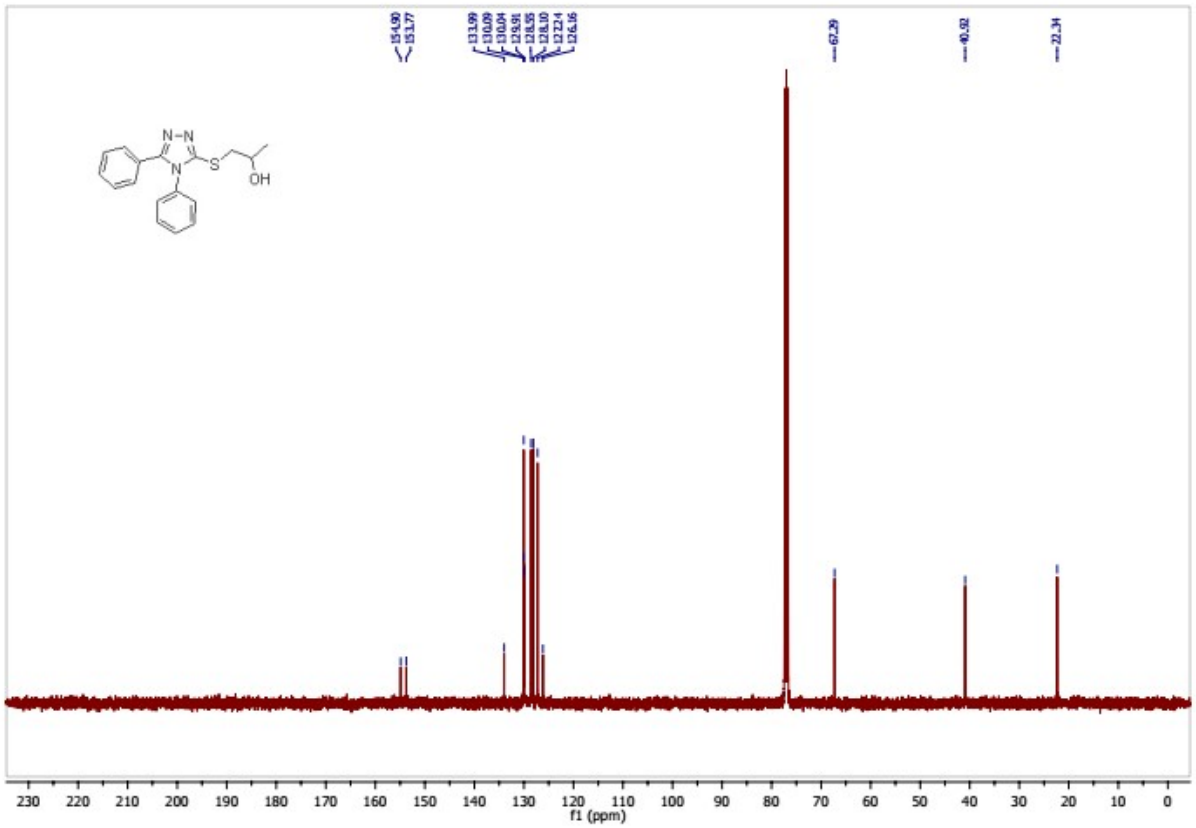

Figure S2: ^{13}C NMR spectrum of 1-((4,5-diphenyl-4*H*-1,2,4-triazol-3-yl)thio)propan-2-ol (**11a**).

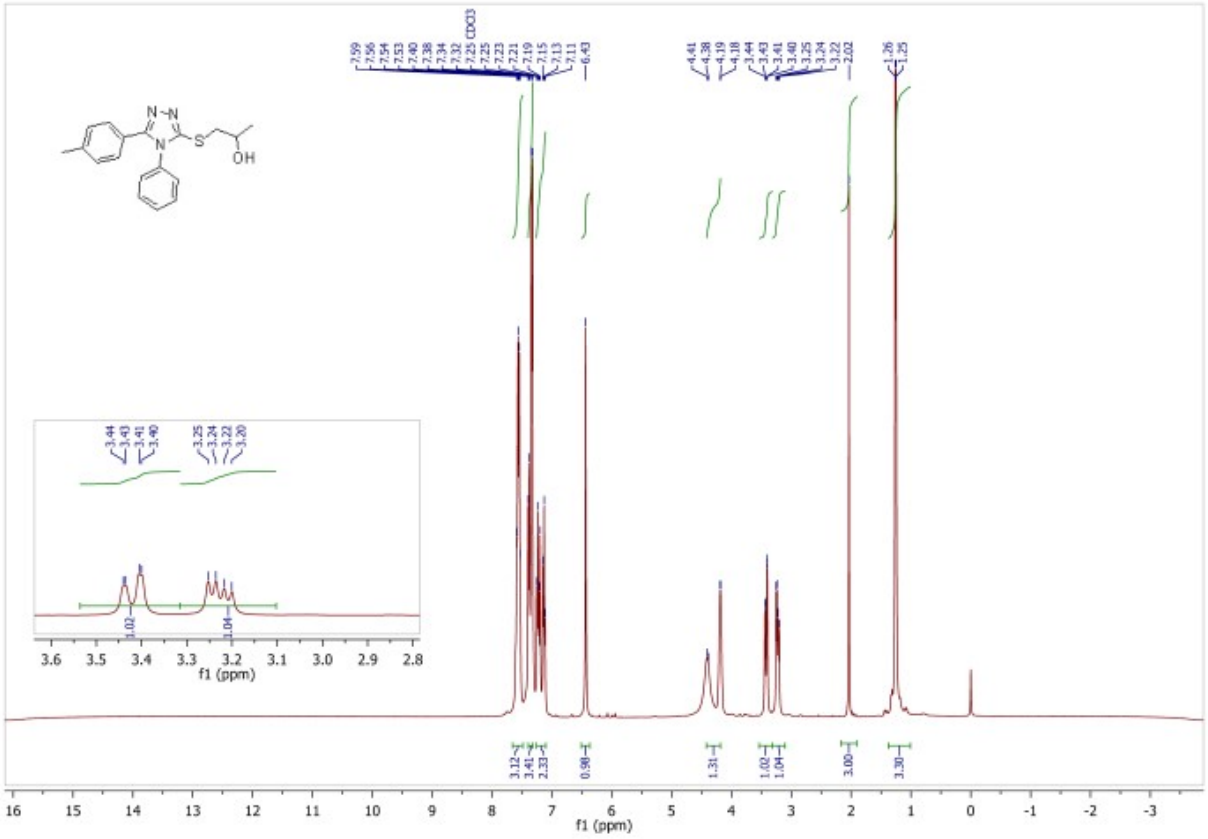

Figure S3: ^{1}H NMR spectrum of 1-((4-phenyl-5-(*p*-tolyl)-4*H*-1,2,4-triazol-3-yl)thio)propan-2-ol (**11b**).

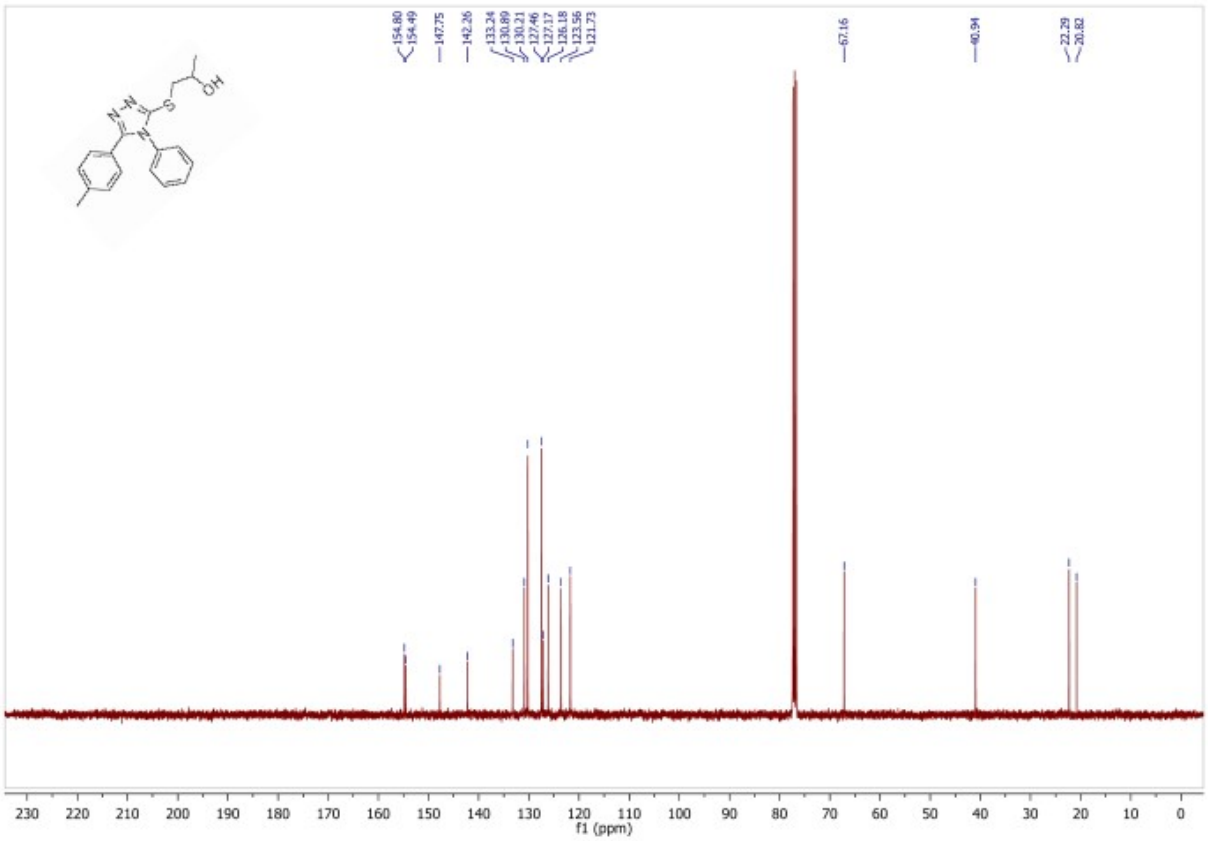

Figure S4: ^{13}C NMR spectrum of 1-((4-phenyl-5-(*p*-tolyl)-4*H*-1,2,4-triazol-3-yl)thio)propan-2-ol (**11b**).

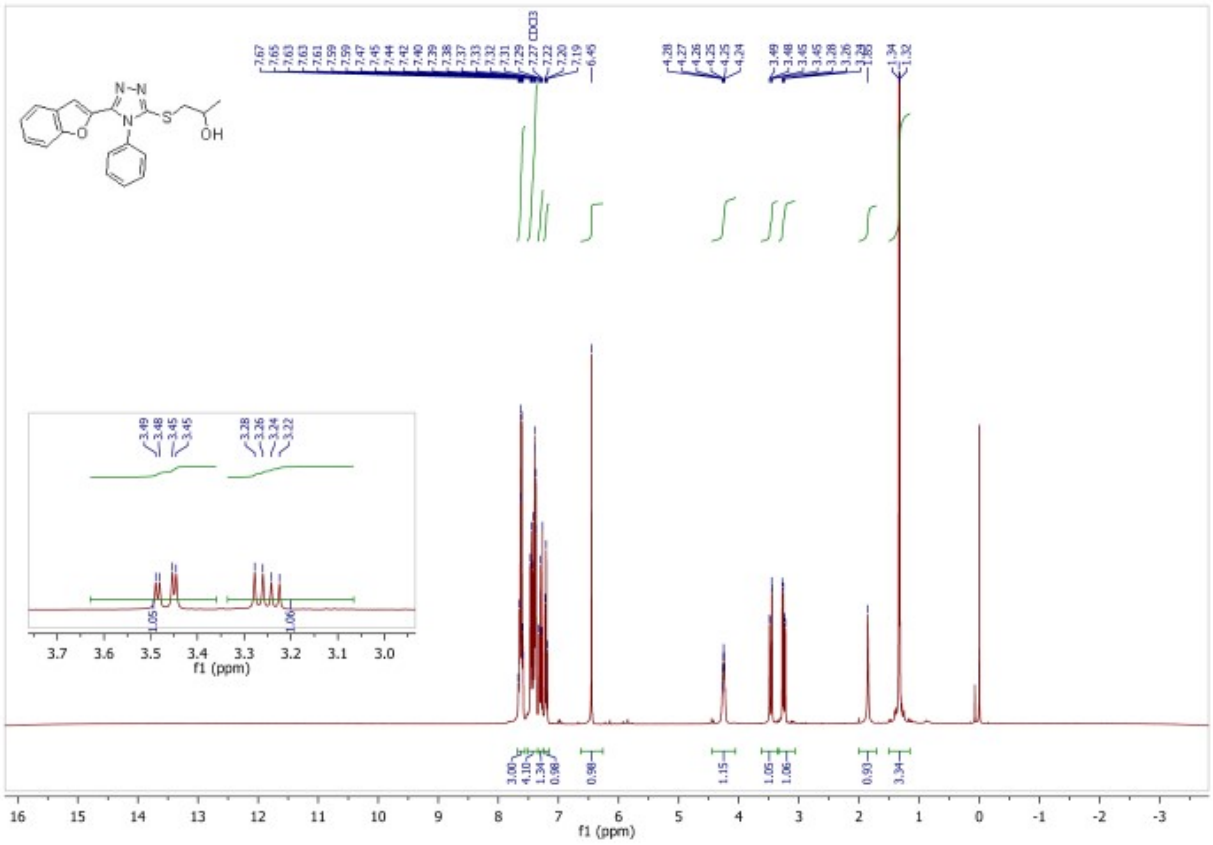

Figure S5: ^{1}H NMR spectrum of 1-((5-(benzofuran-2-yl)-4-phenyl-4*H*-1,2,4-triazol-3-yl)thio)propan-2-ol (**11c**).

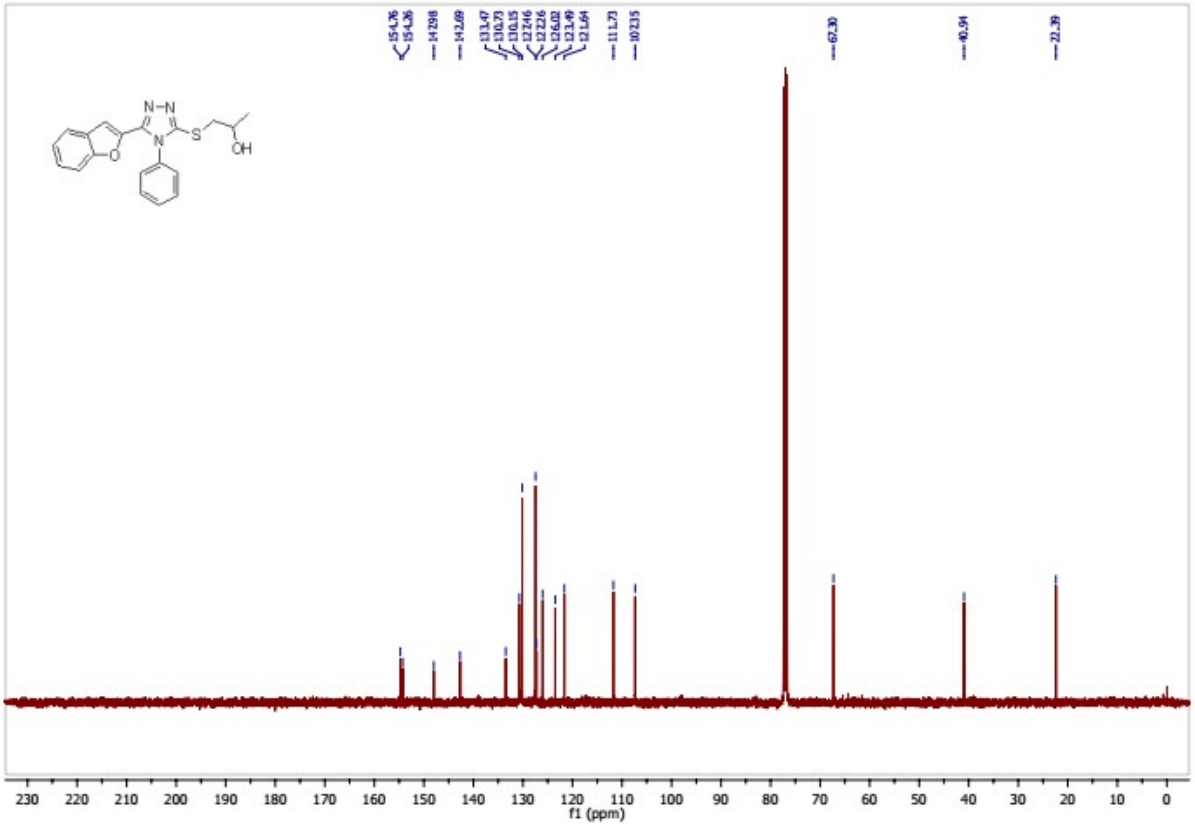

Figure S6: ^{13}C NMR spectrum of 1-((5-(benzofuran-2-yl)-4-phenyl-4*H*-1,2,4-triazol-3-yl)thio)propan-2-ol (**11c**).

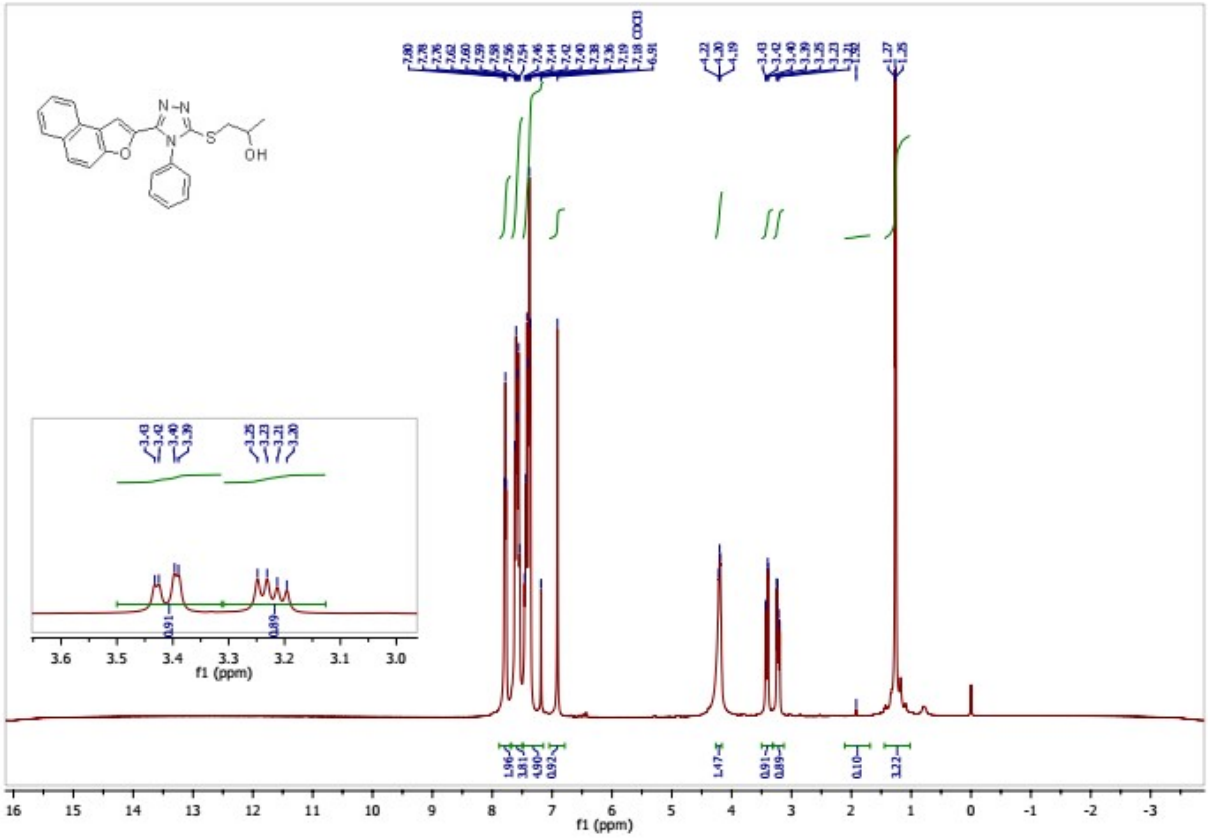

Figure S7: ^{1}H NMR spectrum of 1-((5-(naphtho[2,1-*b*]furan-2-yl)-4-phenyl-4*H*-1,2,4-triazol-3-yl)thio)propan-2-ol (**11d**).

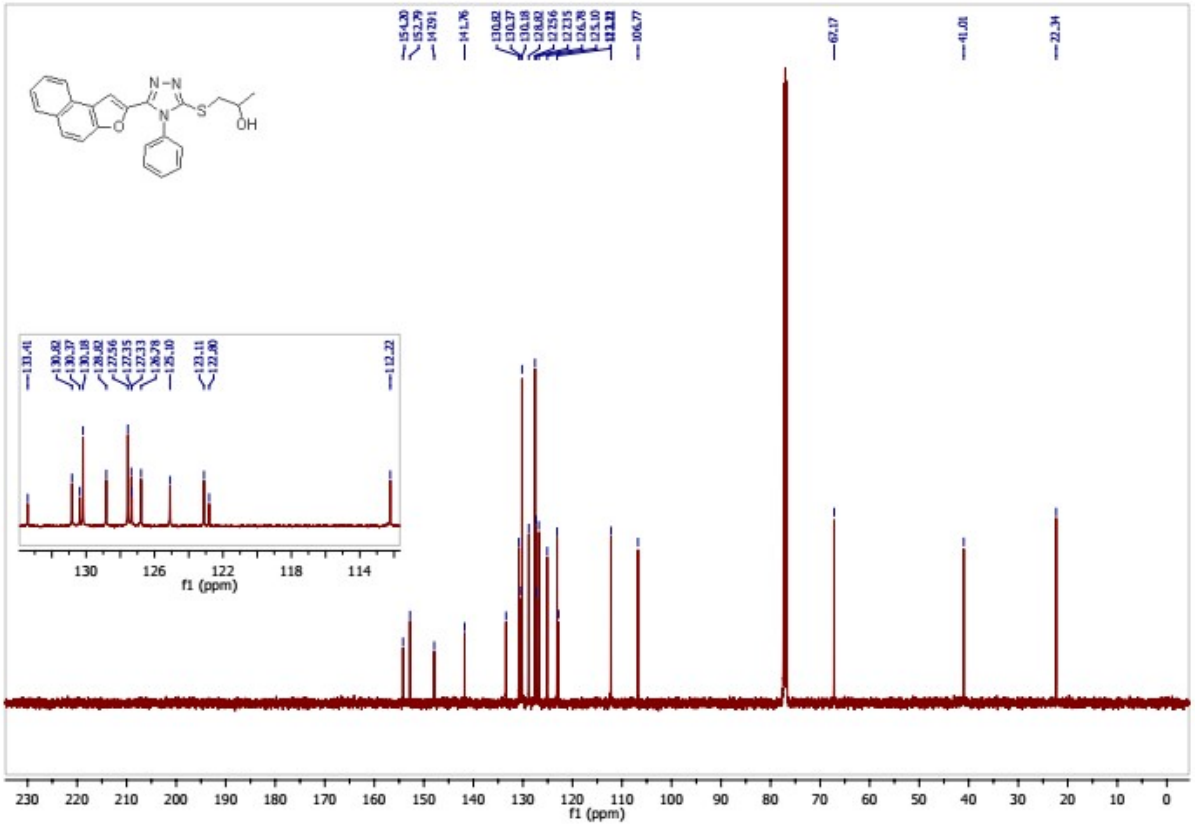

Figure S8: ^{13}C NMR spectrum of 1-((5-(naphtho[2,1-*b*]furan-2-yl)-4-phenyl-4*H*-1,2,4-triazol-3-yl)thio)propan-2-ol (**11d**).

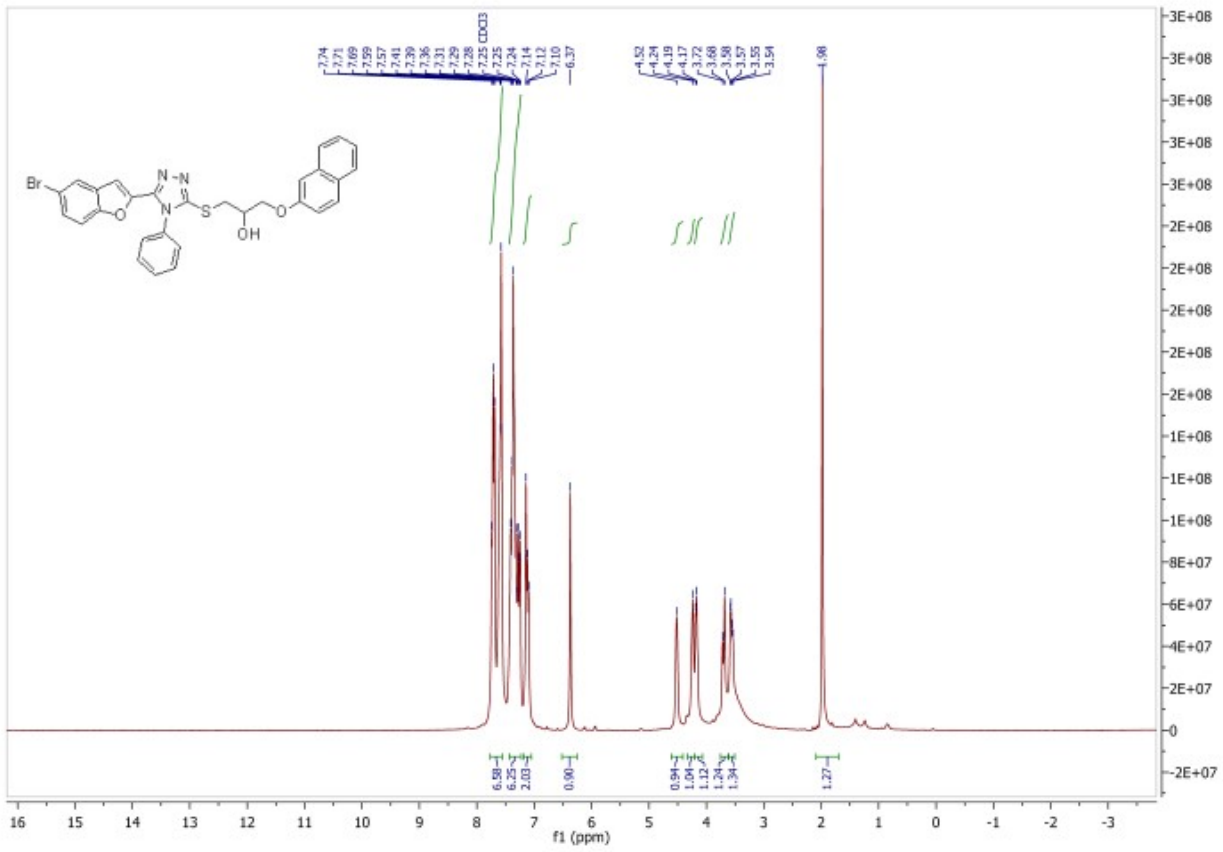

Figure S9: ^{1}H NMR spectrum of 1-((5-(5-bromobenzofuran-2-yl)-4-phenyl-4*H*-1,2,4-triazol-3-yl)thio)-3-(naphthalen-2-yloxy)propan-2-ol (**11e**).

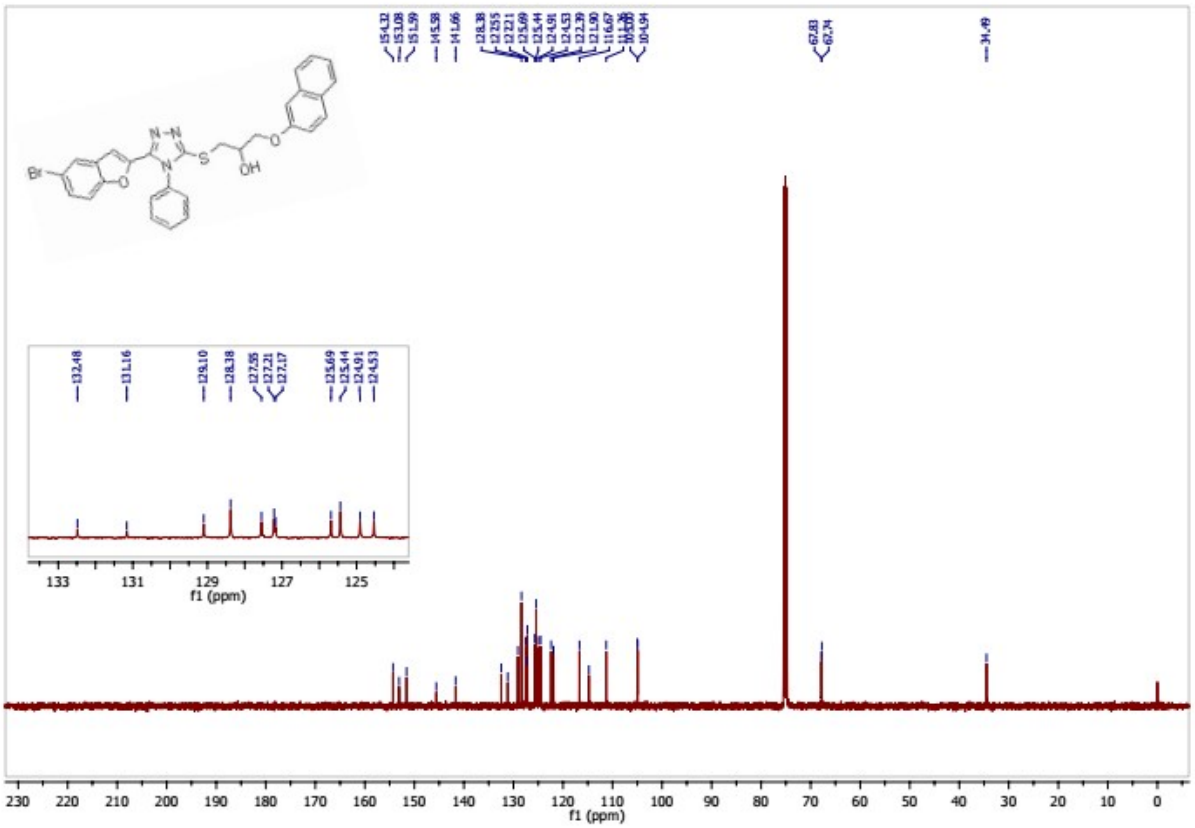

Figure S10: ^{13}C NMR spectrum of 1-((5-(5-bromobenzofuran-2-yl)-4-phenyl-4*H*-1,2,4-triazol-3-yl)thio)-3-(naphthalen-2-yloxy)propan-2-ol (**11e**).

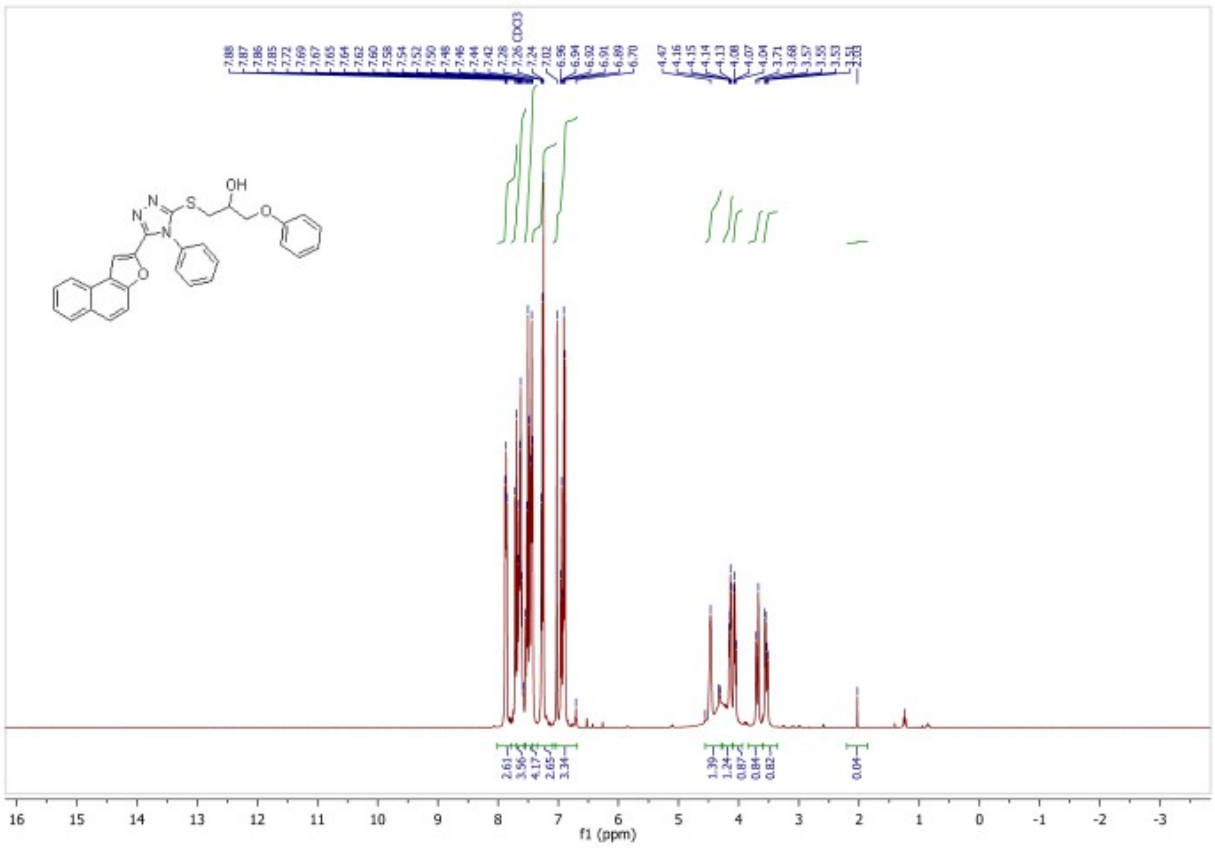

Figure S11: ^{1}H NMR spectrum of 1-((5-(naphtho[2,1-*b*]furan-2-yl)-4-phenyl-4*H*-1,2,4-triazol-3-yl)thio)-3-phenoxypropan-2-ol (**11f**).

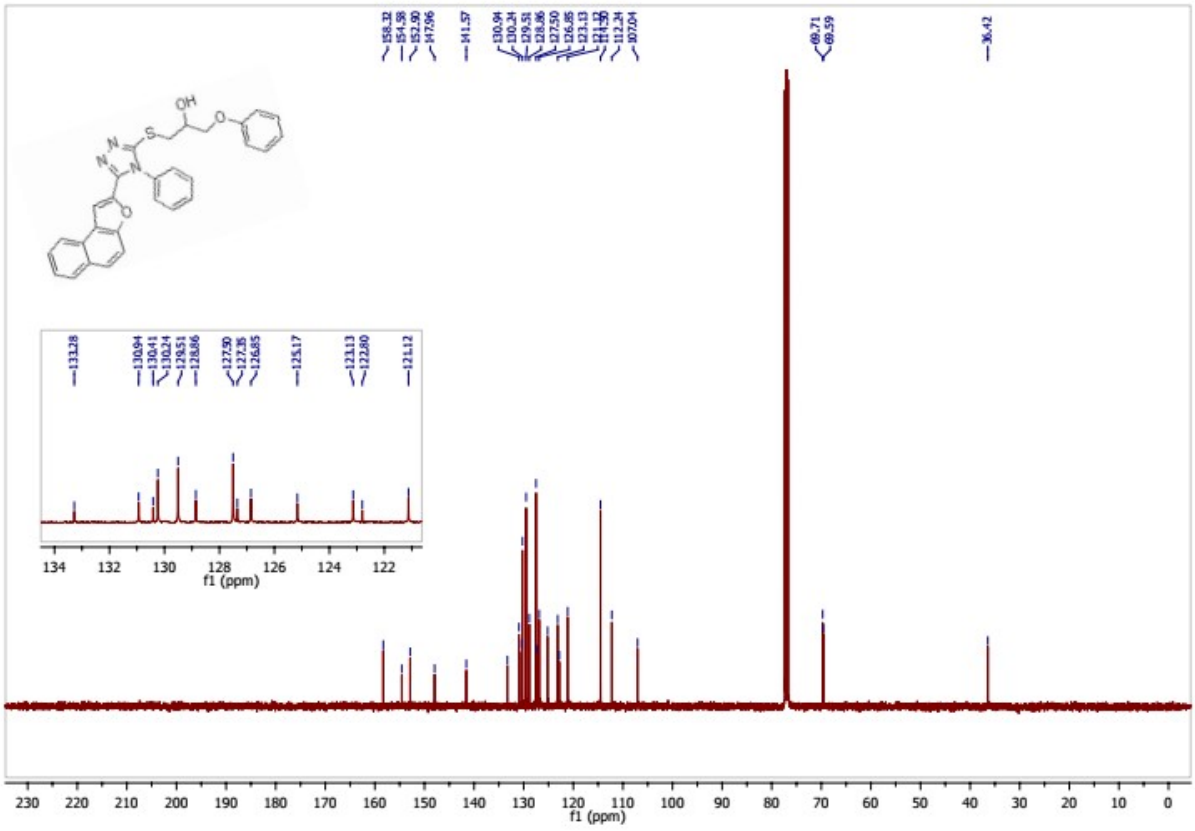

Figure S12: ^{13}C NMR spectrum of 1-((5-(naphtho[2,1-*b*]furan-2-yl)-4-phenyl-4*H*-1,2,4-triazol-3-yl)thio)-3-phenoxypropan-2-ol (**11f**).

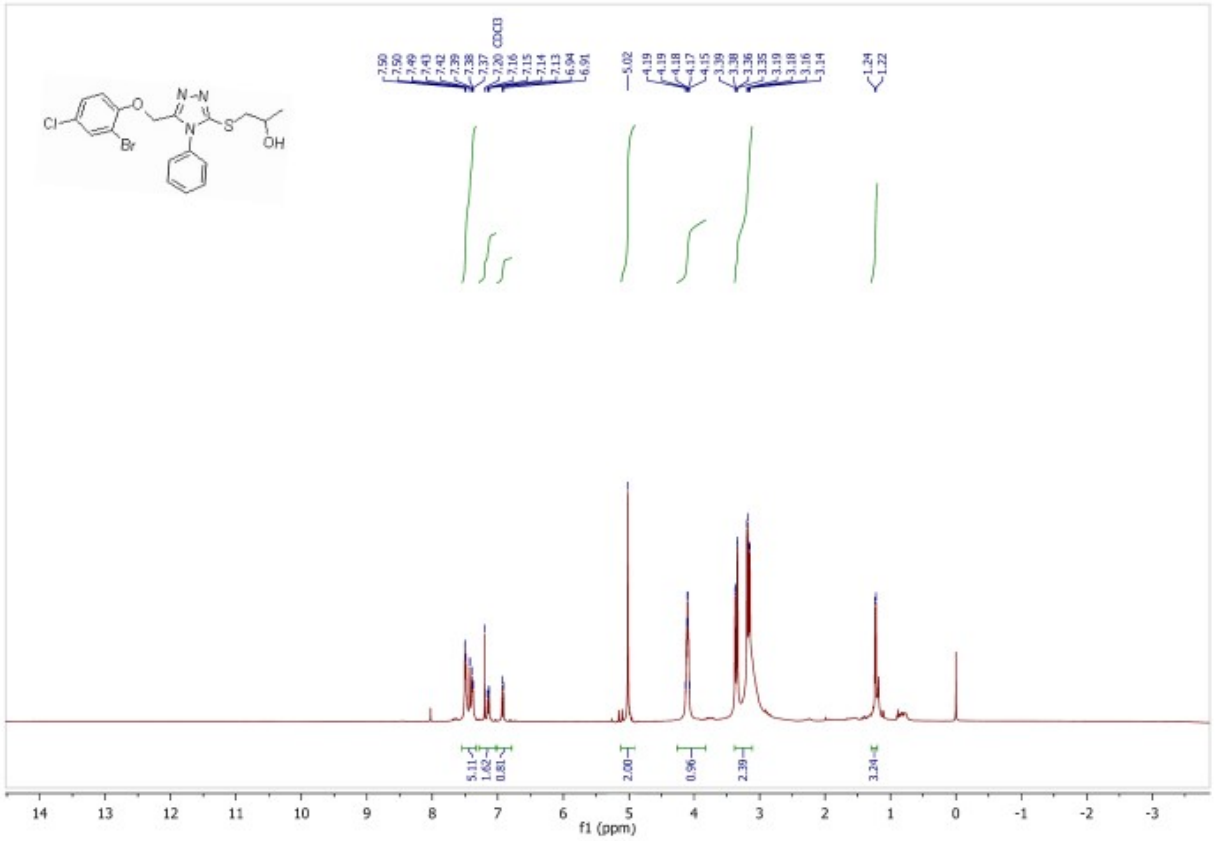

Figure S13: ^{1}H NMR spectrum of 1-((5-((2-bromo-4-chlorophenoxy)methyl)-4-phenyl-4*H*-1,2,4-triazol-3-yl)thio)propan-2-ol (**11g**).

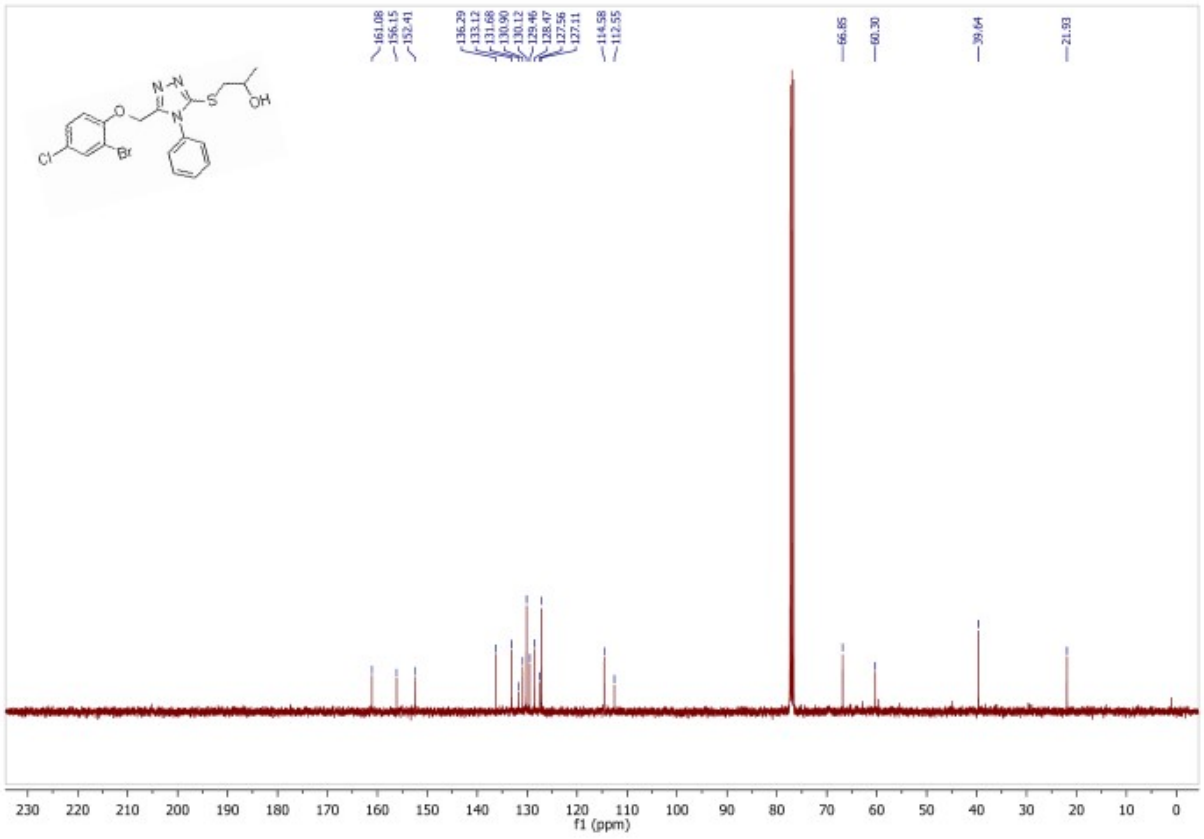

Figure S14: ^{13}C NMR spectrum of 1-((5-((2-bromo-4-chlorophenoxy)methyl)-4-phenyl-4*H*-1,2,4-triazol-3-yl)thio)propan-2-ol (**11g**).

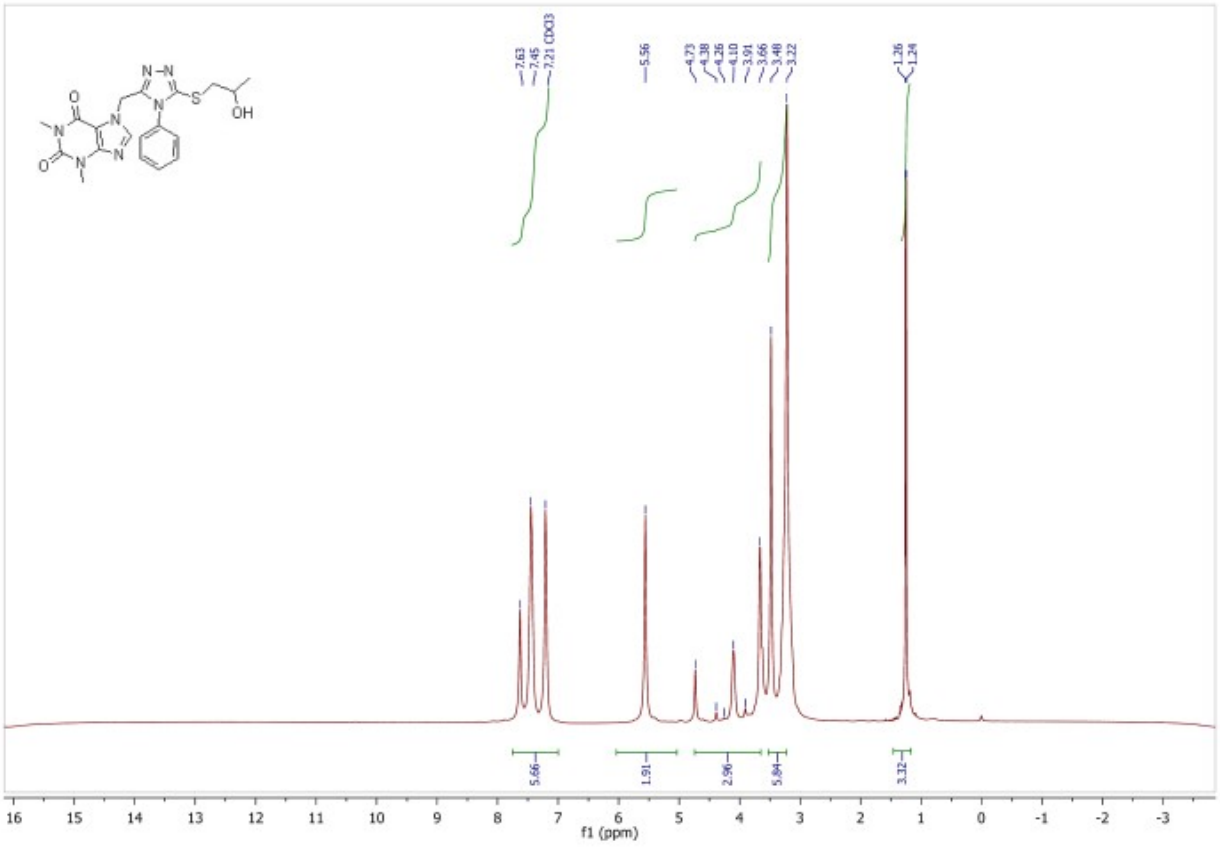

Figure S15: ^{1}H NMR spectrum of 7-((5-((2-hydroxypropyl)thio)-4-phenyl-4*H*-1,2,4-triazol-3-yl)methyl)-1,3-dimethyl-1*H*-purine-2,6(3*H*,7*H*)-dione (**11h**).

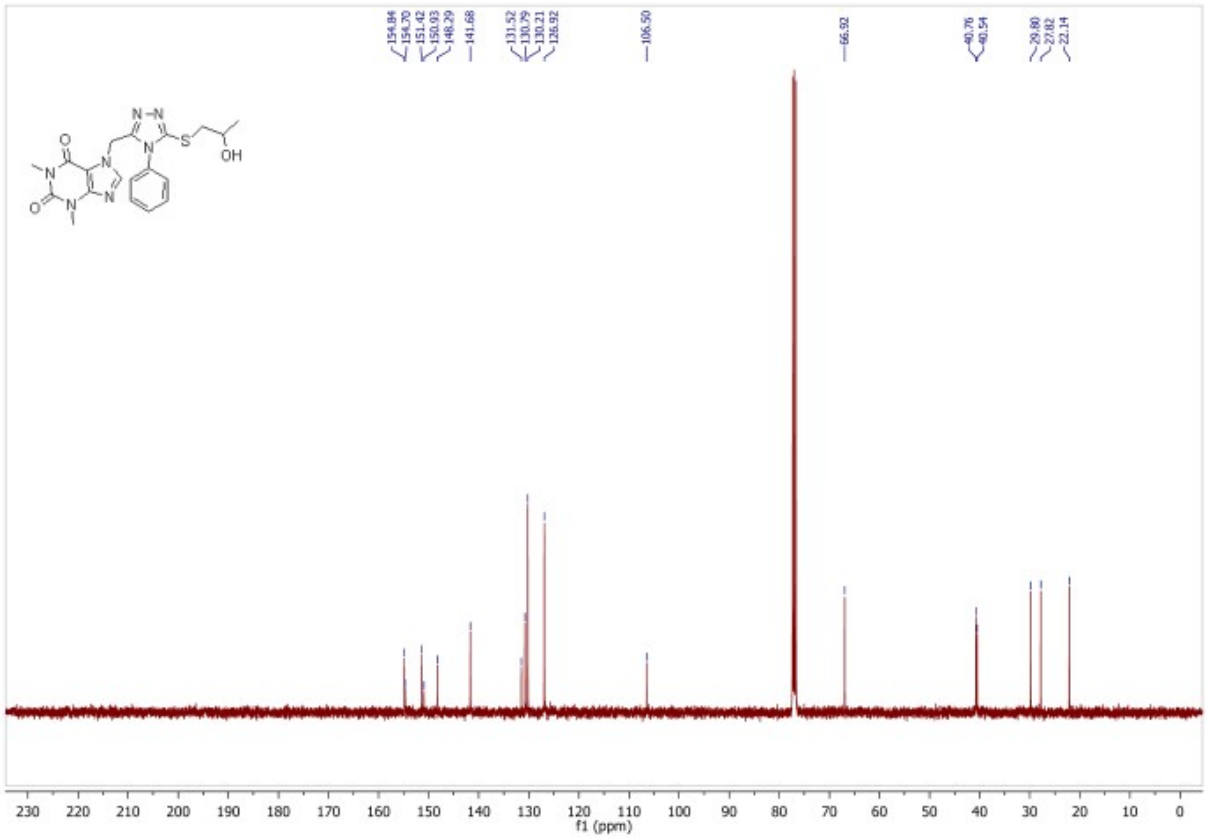

Figure S16: ^{13}C NMR spectrum of 7-((5-((2-hydroxypropyl)thio)-4-phenyl-4*H*-1,2,4-triazol-3-yl)methyl)-1,3-dimethyl-1*H*-purine-2,6(3*H*,7*H*)-dione (**11h**).

2- Bacterial tyrosinase enzyme data

Tyrosinase production and partial purification

Bacterial tyrosinase was produced in a 250 mL flask containing 100 mL following the reported methods of Sharma et al. (2006). The culture supernatant after 65% saturation was centrifuged (10,000×g) at 4°C for 15 minutes. The pellet after resuspending in tris buffer (0.1M; pH 6.8) was dialyzed for 24h at 4°C. The dialysate was loaded onto a Sepharose (anion exchange) column , which was pre-equilibrated and rinsed with Tris–HCl (20 mM, pH 6.0), and absorbed proteins were allowed to elute with a stepwise NaCl gradient in the range of 0.0–1.0 M at a flow rate of 1.0 mL/min. The activity of enzymes was measured using L-tyrosine as a substrate. The results are based on three trials. Bradford's method was used to determine the protein content, which used Bovine Serum Albumin (BSA) as a reference protein (Raval et al., 2014)

Characterization of Tyrosinase

The influence of pH (2 to 10) was determined by using buffers such as Sodium citrate/ citrate acid (pH 2-4) Sodium acetate/ acetic acid (pH 4-6) Sodium phosphate/ phosphoric acid (pH6-8) Ammonium chloride/ ammonium hydroxide (pH 10-). To determine the effect of temperature, the activity of tyrosinase was measured in the temperature range of 30–70 °C using optimum pH to determine the optimal temperature for the preparation (Amin et al, 2010).

Kinetic constants

Kinetic constants were determined by varying concentrations of tyrosine and L-DOPA (0 to 20 mM) and the rates were measured using the linear portion of the absorbance versus concentration curves. The Wilkinson method was used in the Enzpack software to evaluate kinetic constants using non-linear regression analysis (Biosoft, Cambridge, UK). The Km and Vmax values were calculated using Lineweaver–Burk reciprocal plots (Graph-Pad Prism 6 software) based on the results obtained. (Dalfard et al., 2006; McMahon et al., 2007; Selinheimo et al., 2007; Amin et al, 2010)

$$k_{cat} = V_{max} / [E]$$

Results and Discussion

Table1 shows an overview of tyrosinase purification.

Sr. No.	Purification Steps	Total Vol. (mL)	Total Enzyme Activity (IU)	Total Protein Contents (mg)	Specific Activity (U/mg)	Yield (%)	Purification Fold

1	Crude Enzyme	100	469	401	1.15	100	1
2	$(NH_4)_2SO_4$ precipitation	30	324	160	2.025	69	1.76
3	Membrane Dialysis	12	301	88	3.42	64.73	2.97
4	Anion Exchange Chromatography	10	273	69	3.43	58.70	2.98

Influence of pH and temperature on tyrosinase

Using L-tyrosine as a substrate at 30 C °, the effect of pH on the isolated enzyme was examined over a pH range of 2- 10. Results in presented in Figure 1 indicated the influence of pH and temperature. (Dalfard et al., 2006; McMahon et al., 2007; Selinheimo et al., 2007)

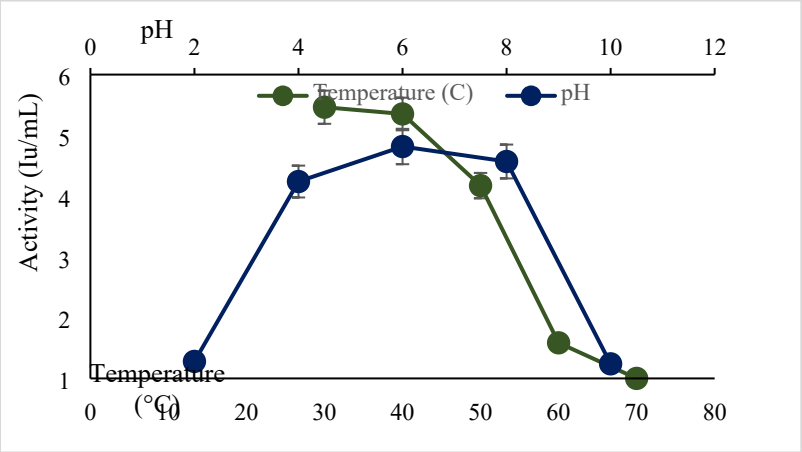

Effect of pH Enzyme

The enzyme was entirely stable below 50°C, but lost its activity quickly once it reached 70°C. Tyrosinases from other sources, such as P. putida F6 and T. reesei, have an optimal temperature of 30°C. (Dalfard et al., 2006; McMahon et al., 2007; Selinheimo et al., 2007)

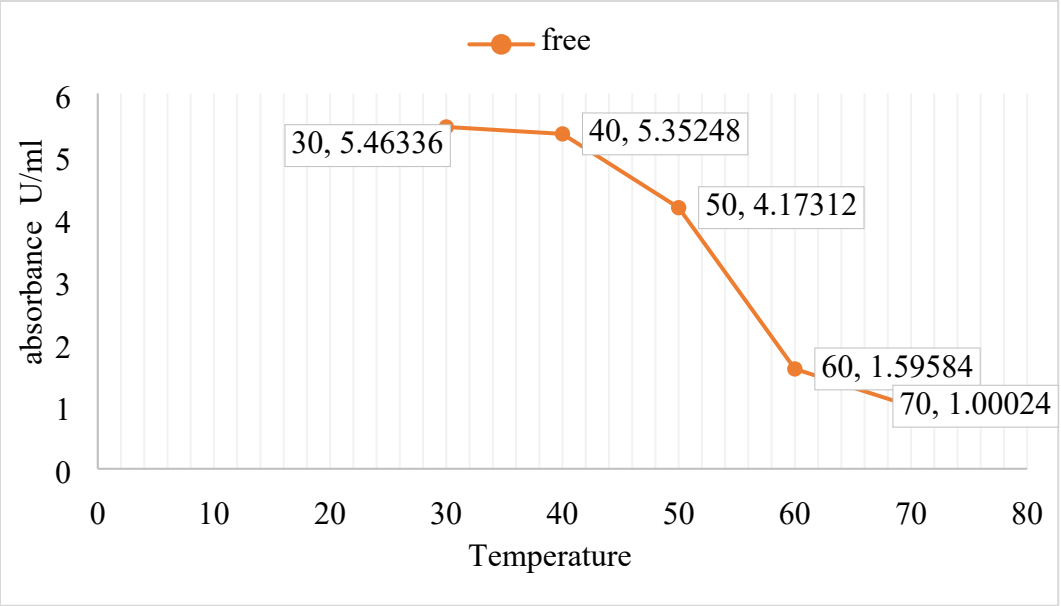

Influence of Temperature and pH on tyrosinase

Determination of kinetic constants

Despite their ability to form associations with a wide range of substrates, the majority of tyrosinases exhibited a stronger affinity for L-tyrosine and L-DOPA as substrates. Bacterial tyrosinase followed Michaelis-Menten kinetics with 0.25mM K_M for L-tyrosine whereas 0.16mM K_M for L-DOPA. (Zdarta et al., 2020)

References:

Amin, E., Saboury, A., Mansouri-Torshizi, H., Zolghadri, S., & Bordbar, A. K. (2010). Evaluation of p-phenylene-bis and phenyl dithiocarbamate sodium salts as inhibitors of mushroom tyrosinase. *Acta Biochimica Polonica*, *57*(3), 277-283.

Dalfard, A. B., Khajeh, K., Soudi, M. R., Naderi-Manesh, H., Ranjbar, B., & Sajedi, R. H. (2006). Isolation and biochemical characterization of laccase and tyrosinase activities in a novel melanogenic soil bacterium. *Enzyme and Microbial Technology*, *39*(7), 1409-1416

McMahon, A. M., Doyle, E. M., Brooks, S., & O'Connor, K. E. (2007). Biochemical characterisation of the coexisting tyrosinase and laccase in the soil bacterium Pseudomonas putida F6. *Enzyme and Microbial Technology*, *40*(5), 1435-1441.

Raval, V. H., Pillai, S., Rawal, C. M., & Singh, S. P. (2014). Biochemical and structural characterization of a detergent-stable serine alkaline protease from seawater haloalkaliphilic bacteria. *Process Biochemistry*, *49*(6), 955-962.

Selinheimo, E., Autio, K., Kruus, K., & Buchert, J. (2007). Elucidating the mechanism of laccase and tyrosinase in wheat bread making. *Journal of Agricultural and Food Chemistry*, *55*(15), 6357-6365.

Sharma AD, Kainth S, Gill PK. Inulinase production using garlic (Allium sativum) powder as a potential substrate in Streptomyces sp. J Food Eng, 2006; 77:486-491.

Zdarta, J., Staszak, M., Jankowska, K., Kaźmierczak, K., Degórska, O., Nguyen, L. N., ... & Jesionowski, T. (2020). The response surface methodology for optimization of tyrosinase immobilization onto electrospun polycaprolactone–chitosan fibers for use in bisphenol A removal. *International Journal of Biological Macromolecules*, *165*, 2049-2059.